Crystallization of High-Density Polyethylene–Linear Low-Density Polyethylene Blend

S. K. RANA*

Department of Textile Technology, Indian Institute of Technology, New Delhi-110016, India

Received 16 July 1997; accepted 16 January 1998

ABSTRACT: The crystallization studies revealed that the high-density polyethylene (HDPE) and linear low-density polyethylene (LLDPE) formed strong cocrystalline mass when they were melt blended in a single screw extruder. The progress of crystallization was observed through a small-angle light scattering instrument, scanning electron microscope, and differential scanning calorimeter. Analysis showed that these constituents followed individual nucleation and combine growth of crystallites in blends. The growth of crystallites all through the blend compositions were two-dimensional. Interestingly, the crystallites resembled each other for a particular blend composition; however, they differ widely as the composition changes. The rate of crystallization depends greatly to the number of crystallites and their interfacial boundary in contact with the amorphous phase pool. The $t_{1/2}$ and percentage of crystallinity showed a mutually exclusive trend and were seen to be varied in the following three regions of blend composition: the HDPE-rich, the LLDPE-rich, and the middle region of blend composition. The percentage of crystallinity decreases in both the HDPE-rich and LLDPE-rich blends, and it showed a plateau value in the middle region of blend composition. The $t_{1/2}$ showed opposite trend to that of % crystallinity. © 1998 John Wiley & Sons, Inc. J Appl Polym Sci 69: 2599–2607, 1998

Key words: crystallization; morphology; cocrystallinity; crystallites

INTRODUCTION

There is a rather strange behavior in the compatibility of polyethylenes among themselves. Some grades are compatible with few selective grades, while with other grades, they are incompatible. Perhaps this is one of the most important reasons why the superior mechanical properties of high-density polyethylene (HDPE), and the excellent heat sealability of low-density polyethylene (LDPE) could not be incorporated in a single mass through blending. These properties are extremely important for the use of polyethylene as a commodity plastics. However, these properties are engineered in the youngest and commercially important linear low-density polyethylene (LLDPE). Besides, it also possesses good environmental stress cracking resistance and thin film-forming properties. Furthermore, the LLDPE manifests good compatibility to both the HDPE and LDPE, which leaves enough scope for tailoring desirable properties in the blends.

Considering that they all are derived from the ethylene monomer through different polymerization techniques and/or incorporating a small amount of comonomer, namely, octene and hexene and that the resulting polymers are almost structurally similar, it is difficult to understand their causes of incompatibility. The incompatibility arising out of the amorphous phase sounds unrealistic because of looseness of its construc-

* *Present address:* F-27 Jia Sarai, Hauz Khas, New Delhi, 110 016, India.

Journal of Applied Polymer Science, Vol. 69, 2599–2607 (1998)
 CCC 0021-8995/98/132599-09

Table I Characteristic Properties of HDPE and LLDPE

Properties	HDPE	LLDPE
[n] at 115°C in decalin (dL/g)	1.10	1.50
T_m (°C)	131	126
Melt flow index (g/10 min)	0.75	1.00
Density (g/cc)	0.952	0.925
Tensile at yield (MPa)	24.5	19.3
CH_3–100 carbon atom	1.81	3.00
Crytallinity (%)	46	36

tion, and it can accommodate entanglements, chain ends, and pendent groups. In the absence of any major compulsive force among chain segments in the amorphous phase, the compatibility among polyethylenes may be viewed as the extent of accommodativeness of their chain segments in the crystalline phase. As the crystalline phase is considered to be very ordered and selective in accommodating linear chain segments, a slightest variation in chemical structure of the polyethylene segments partaking crystallization is rejected by the crystalline phase and results in the formation of individual crystalline phase and/or segregation to its constituents. When the polyethylene chain sequences of both the constituents undergo crystallization in a single crystalline entity, cocrystallization results.[1–3] Furthermore, the occurrence of cocrystallization ought to have an effect on the structural conformation of crystallites. In this article, the effect of cocrystallization on the nucleation, growth of crystallites, and its kinetics is explored.

EXPERIMENTAL

Materials

The HDPE (Hostalene GF7745F) used for this study was a product of Polyolefin Industries Ltd., Bombay, India. The LLDPE (Dowlex 2740E), an octene-based copolymer, was a product of Dow Chemicals, U.S.A. The properties of these two pure polymers are listed in Table I.

Blend Preparation

The granuels of HDPE and LLDPE were mixed in a tumble mixer so as to form a uniform composition all through the batch size. These uniformly mixed polyethylene batches were then melt-blended in a single screw extruder (Betol 1820, U.K.) with an L/D ratio of 17 and a screw speed of 22 rpm. The temperature profile of the extruder was kept as 160, 200, and 210°C at the fed zone, compression zone, and metering zone, respectively. The die end was kept at 200°C. The extruded strands were cooled in water bath maintained at 30°C, and, subsequently, they were granulated after allowing a maturation time of 8 h.

Compression Molding

The compression molding was done at (165 ± 2)°C and at a pressure of 300 kg/cm^2 for 2 min, followed by solidification under nominal pressure for another 2 min. The films so obtained were quenched in water at 30°C. These films were used for differential scanning calorimetric study, small-angle light scattering experiment, and chlorosulphonic acid etching.

Measurements

Small-Angle Light Scattering Experiment

The thin compression molded films were used for this "Hv" light scattering experiment. The scattering patterns were recorded in flat plate photographic films without disturbing the distance between the source, sample, and photographic film in all the cases. The Hv designates the direction of the polarizer and analyzer with one in the horizontal and the other in the vertical position.

Scanning Electron Microscopy

Compression molded films of selective compositions were etched in chlorosulphonic acid at room temperature for 24 h. The etched films were washed thoroughly in distilled water and dried. These films were then shaded by gold by vacuum deposition technique and were photographed in a scanning electron microscope (Cambridge instrument, Stereoscan 360, U.K.), keeping the tilt angle at zero.

Differential Scanning Calorimeter

The powdered sample weighing about 10 mg was taken in an aluminum crucible and crimped for the differential scanning calorimetry (DSC) experiment in a Perkin–Elmer DSC-7 thermal system, U.S.A. The samples were heated to 165°C and kept for 2 min under a nitrogen blanket. The molten mass was then rapidly cooled to 115°C

and held isothermally at this temperature to obtain traces of crystallization exotherm. The percentage of crystallinity is calculated as

$$\text{Crystallinity } (X\%) = [\delta H/\delta H_c] \times 100$$

where ΔH is the heat of crystallization of the sample, and ΔH_c is the heat of crystallization of 100% crystalline polyethylene. The seeding time (t_{seeding}) is defined as the time at which the molten mass starts forming nuclei and is evaluated as the intersection between the base line and the tangent to the lower time side of the exothermic peak (shown in Fig. 3).

RESULTS AND DISCUSSION

Small-Angle Light Scattering

The Hv scattering patterns of HDPE, LLDPE, and the 50/50 blend are shown in Figure 1. The scattering pattern suggests the presence of sheaflike and/or disklike[4,5] crystallites for all three samples, notwithstanding that there are subtle differences in their scattering patterns. The lobes of HDPE are sharp and the lobes of LLDPE are well defined. The scattering pattern of 50/50 blend may be assumed to be the superimposition of the scattering patterns of these two pure constituents. The scattering patterns of the rest of the blend samples are almost qualitatively similar (not shown in Fig. 1).

Scanning Electron Microscopy

Figure 2(a–e) shows the micrographs of chlorosulphonic acid etched samples of two pure constituents and three of their blends: one with HDPE as the major constituent, the 65% HDPE containing blend; the other with LLDPE as the major constituent, the 80% LLDPE containing blend; and the 50/50 blend. The chlorosulphonic acid etching was reported[6,7] to dissolve the amorphous part; hence, the crystalline part is revealed as it remains on the surface after dissolution of the amorphous phase.

Figure 2(a) shows disklike HDPE crystallites approximately 25 to 50 Å in diameter along with large number of bright dots. Such dots are also present in the microphotographs at all compositions. This sheaflike crystallites[8] with an average dimensions of 500 Å in length and 15 Å in width are seen in the micrograph of LLDPE [Fig. 2(b)].

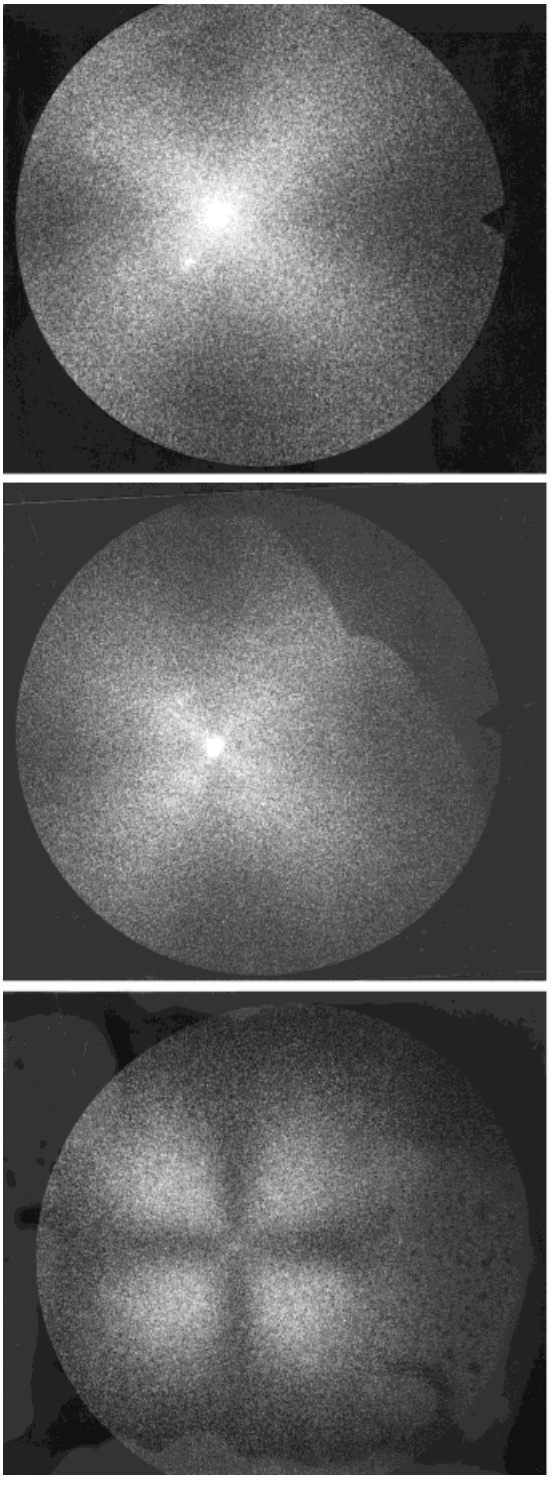

Figure 1 (a–c) Small-angle light scattering pattern of (a) HDPE, (b) 50/50 blend, and (c) LLDPE.

The crystallites of 80% LLDPE containing blend closely match the crystallites' conformation of pure LLDPE, although some interference of

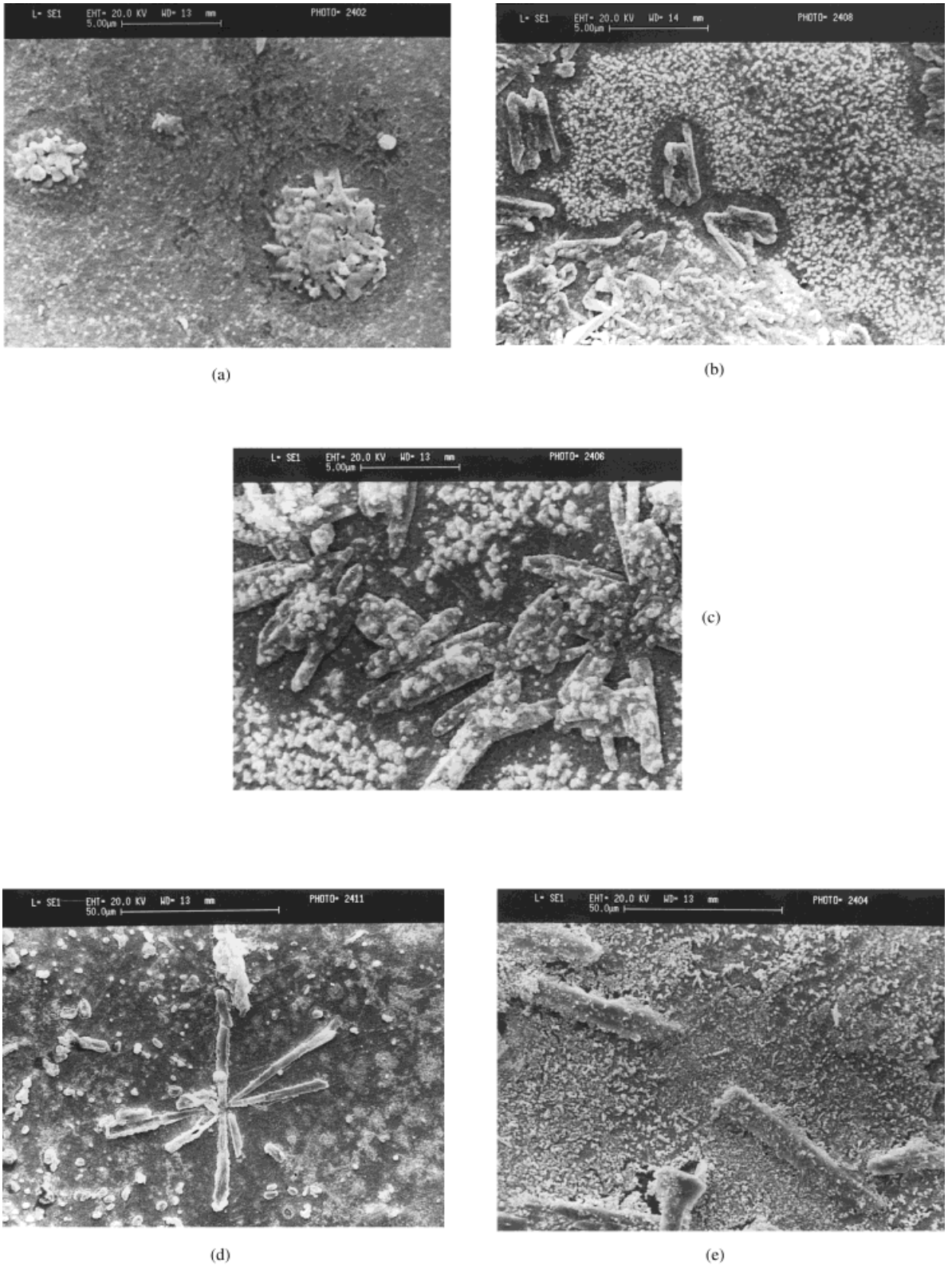

Figure 2 (a–e) Micrographs of cholorosulphonic-acid-etched samples of (a) HDPE, (b) 65/35 HDPE–LLDPE blend, (c) 50/50 blend, (d) 20/80 HDPE–LLDPE blend, and (e) LLDPE.

Table II Isothermal Crystallization Kinetic Parameters of HDPE–LLDPE Blends

Sample Wt % HDPE : LLDPE	Crystallinity	Avrami Exponent (n)	$t_{1/2}$ (min)	$k \times 10^4$ min^{-1}
100 : 0	60.5	3.09	10.88	4.34
90 : 10	57.8	2.75	15.34	3.80
75 : 25	54.8	2.39	19.03	6.06
65 : 35	51.3	2.60	21.33	10.21
50 : 50	51.2	2.30	15.75	12.21
30 : 70	46.3	2.22	24.21	13.05
20 : 80	44.0	2.12	29.29	13.05
0 : 100	37.8	2.05	50.57	2.23

HDPE in them is discernible. The crystallites of 35 and 50% LLDPE-containing blends [Fig. 2(c,d)] are platelike with average dimensions of 50 Å in length and 10 Å in width.

One would appreciate from these micrographs that the growth of crystallites are largely two-dimensional. However, their physical appearance at each composition is unique. Such uniqueness in crystallites structure at different blend compositions may be responsible for their differences observed in the light scattering patterns (see Fig. 1).

Differential Scanning Calorimetry

Figure 3 represents the singlet isothermal crystallization exotherms (ICE) of HDPE and LLDPE, along with some of their selected blends. Some characteristic data of these ICE are presented in Table II. On close examination, Figure 3 reveals

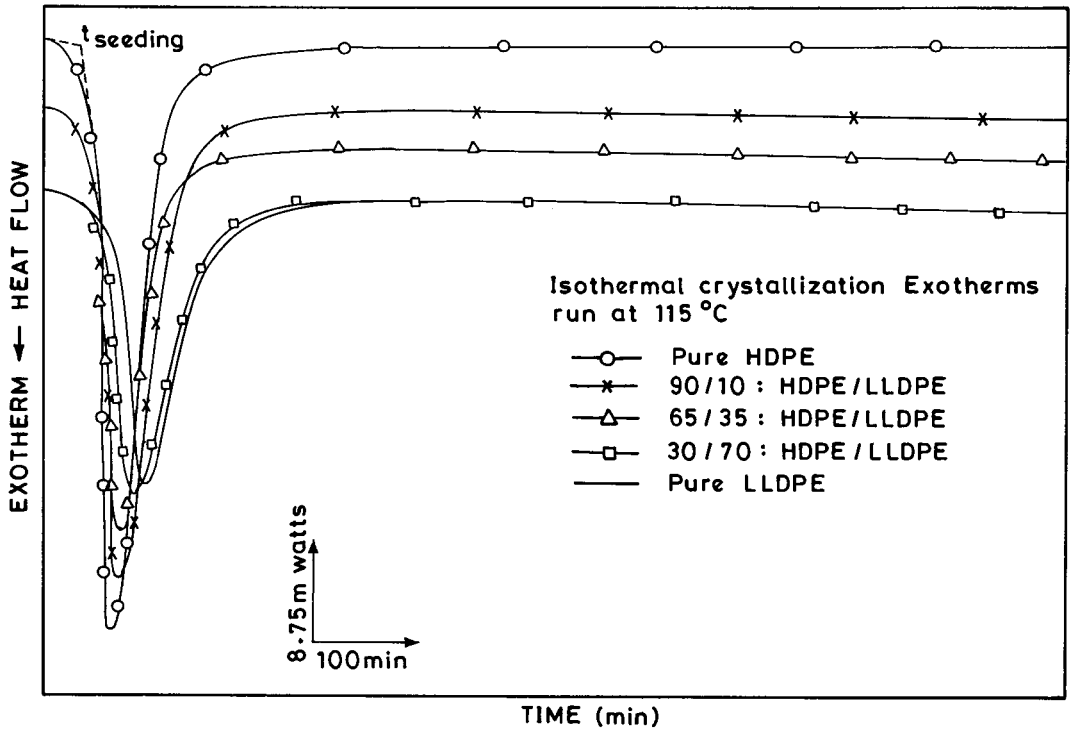

Figure 3 Isothermal crystallization exotherms of HDPE, LLDPE, and some of their selective blends.

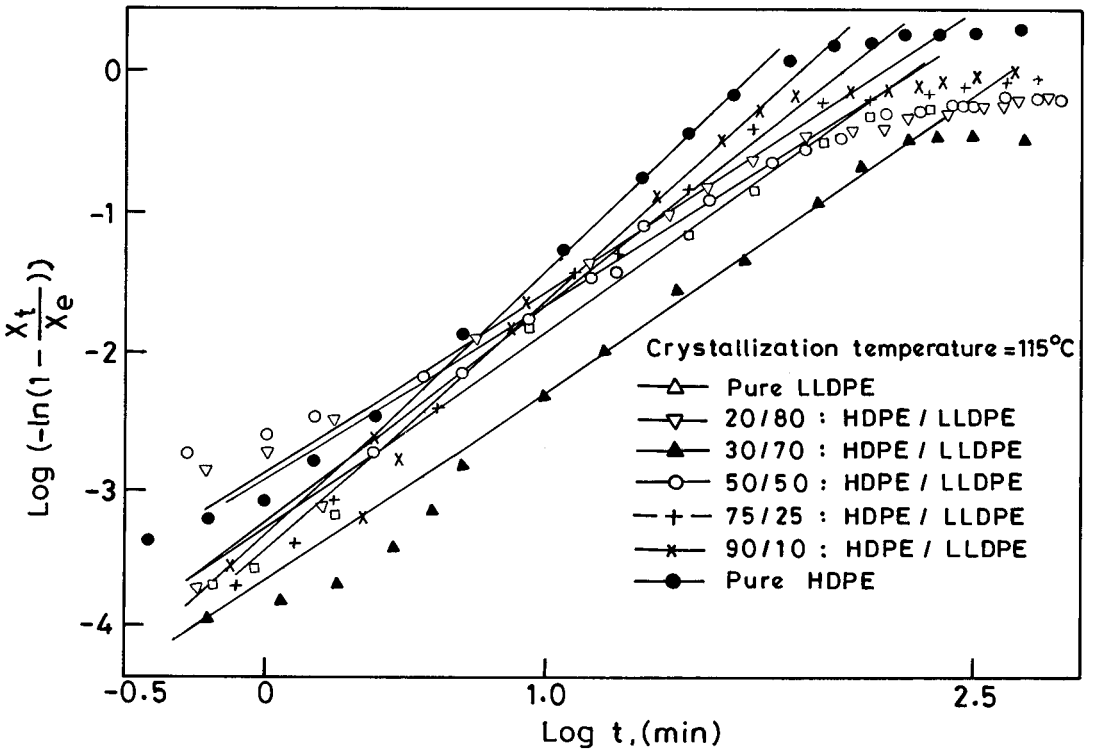

Figure 4 Avrami plots of crystallization parameters of HDPE–LLDPE blends.

that the exothermic peak of HDPE is narrower in width and has a greater area when compared with LLDPE. The ICE of blends closely resemble to the ICE of their major constituent; however, the exothermic peak of 50/50 blend matches the HDPE in peak area and the LLDPE in peak width. As the singlet exothermic peak was attributed to the cocrystallization between HDPE and LLDPE by many authors[1–3] for nonisothermal crystallization process, it is attributed to the cocrystallization between HDPE and LLDPE for this case also. Unlike nonisothermal crystallization in which the faster crystallization rate puts hindrances for the constituents to undergo individual crystallization and phase segregation due to the intimate presence of both HDPE and LLDPE and ultimately underwent cocrystallization, the isothermal crystallization carried out at as a high temperature one at 115°C for prolonged periods would cocrystallize due to the strong affinity between the pure constituents.

The Avrami Plot

The time-dependent crystallinity (X_t), maximum achievable crystallinity (X_e), rate constant (k), and the Avrami exponent (n) bear the relationship[9–14] shown in eq. (1).

$$X_t = X_e\{1 - \exp(-kt^n)\} \quad (1)$$

Equation (1) could be rearranged into the following form (eq. 2):

$$\log[-1n\{1 - (X_t/X_e)\}] = \log(k) + n\ \log(t) \quad (2)$$

Thus, the plot of $\log[-\ln\{1 - (X_t/X_e)\}]$ against $\log(t)$, as per eq. (2), will provide a straight line with slope n and intercept $\log(k)$.

The plot of $\log[-\ln\{1 - (X_t/X_e)\}]$ versus $\log(t)$ is shown in Figure 4. Though most of the points essentially lie in a straight line, some points, particularly at the beginning and the end, deviate from the straight line behavior, which indicates a slow progress of crystallization at the beginning and the end of it. The slow crystallization at the beginning signifies slow seeding of crystallites (nucleation), whereas the slow end is an indicative of the hindered growth of crystallites due to their impingement. Therefore, straight lines are drawn (Fig. 4) to represent the region of unhin-

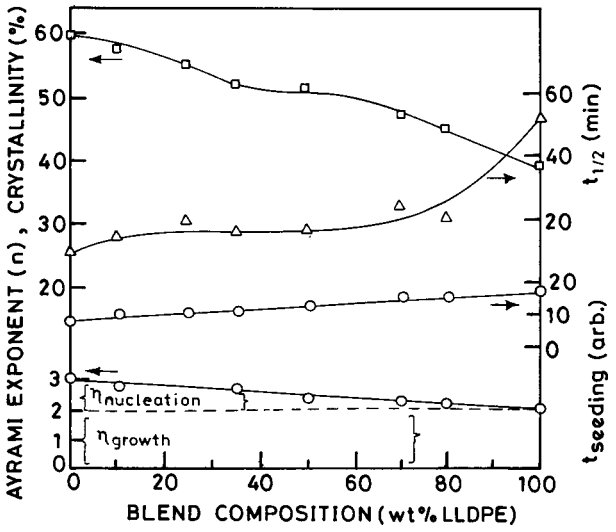

Figure 5 Plot of the percentage of crysallinity, $t_{1/2}$, t_{seeding}, and Avrani exponent as a function of blend composition.

dered growth of crystallites. The Avrami exponent (n), the rate constant (k), and the percentage of crystallinity, together with the half-time of crystallization [$t_{1/2}$, which is equal to $(\ln 2/k)^{1/n}$] are listed in Table II.

Figure 5 shows the dependence of percentage crystallinity, $t_{1/2}$, $t_{seeding}$ (defined in Fig. 3) and the Avrami exponent on blend composition. Approximately, the percentage of crystallinity curve varies in the following three regions of blend composition: The HDPE-rich, the middle region, and the LLDPE-rich region. A rapid decrease in crystallinity from 61 to 51% is seen in the HDPE-rich region with 30% LLDPE content (Fig. 5). The percentage of crystallinity remains constant at the 51% level in the middle region, that is, 30 to 70% range of LLDPE containing region. The decrease in the percentage of crystallinity is also apparent in the 70 to 100% LLDPE-containing region, that is, the LLDPE-rich blend. A point to note is that the percentage crystallinity reported in Table I is nonisothermal crystallinity of the as-obtained samples, scanned at a run rate of 10 degrees per minute and is considerably lower than the isothermal crystallinity. The prolonged period of the isothermal crystallization run perhaps helps these samples to attain higher crystallinity. The mutually exclusive $t_{1/2}$ to that of the percentage of crystallinity is also seen to vary in three regions of blend composition but in the opposite direction. The high value of $t_{1/2}$ hints at the slow crystallizing mass, so the percentage of crystallinity achieved for a given time is lower than the polymer blend with a low $t_{1/2}$ value.

The trend of variation of crystallization rate constant shows little sensitivity to the blend compositions. An increase in rate constant is seen up to 25% LLDPE content from pure HDPE, even though the rate constant of pure LLDPE is lower than the rate constant of HDPE. A steep increase in rate constant could be observed beyond this 25% LLDPE content, which is maintained up to 80% LLDPE containing blend with a sharp drop of it with pure LLDPE. The number and size of crystallites (see Fig. 2) increased sharply in the 25 to 80% LLDPE-containing blends. Hence, a large crystal growth front is available for the amorphous phase pool to undergo crystallization and the crystallization proceeds faster. The crystallization rate constant in this region increases accordingly.

The Avrami exponent is fractional (see Table II) for blends, as well as their pure constituents. At the present level of understanding,[15–18] the integral value of Avrami exponent is accepted for both the polyethylenes, which was attributed to the different types of seeding and growth of crystallites. This holds good for two pure constituents. On rounding up, the Avrami exponent becomes 2 for LLDPE and 3 for HDPE. The Avrami exponent of 2 for LLDPE was ascribed to either the sporadic nucleation and rodlike growth or the instantaneous nucleation and sheaflike growth of crystallites, whereas the Avrami exponent of 3 for HDPE to the sporadic nucleation and disklike growth or to the instantenous nucleation and spherulitic type growth of crystallites. However, the Avrami exponent is distinctly fractional for blends. These fractional values could be considered as being made up in different combinations of these two extremes 2 and 3 of Avrami exponent for LLDPE and HDPE, respectively.

The SEM micrographs [see Fig. 2(a–e)] showed two-dimensional growth of crystallites in all the cases. Thus, an integral value of 2 from the Avrami exponent could be set aside, signifying the two-dimensional growth of crystallites and is represented here as n_{growth}. The remaining part 0 for LLDPE and 1 for HDPE of the Avrami exponent may be attributed to the instantaneous nucleation and sporadic nucleation of crystallites for LLDPE and HDPE, respectively. A systematic shift from instantaneous nucleation to the sporadic nucleation of the blends, as the LLDPE content decreases, is perhaps responsible for their fractional value of Avrami exponent. The combi-

nations of 0 and 1 in appropriate proportions may account for the fractional values of Avrami exponent over the integral value of 2, indicating the growth of crystallites. This fractional part of Avrami exponent is represented here as $n_{nucleation}$. The linear change in $t_{seeding}$ (Fig. 5) with blend composition reinforces the belief of systematic variation of the types of seeding of crystallites as the blend composition changes.

Thus the Avrami exponent (n) may thus be assumed to be comprised of two parts, which are related as

$$n = n_{nucleation} + n_{growth}$$

where the n_{growth} is blend-composition-independent part, and the $n_{nucleation}$ is blend-composition-dependent part. The Avrami exponent (n) for the entire blend composition is plotted in Figure 5, depicting these partitioned values.

For cocrystallization to occur, the constituting components would either have common nucleation or common growth of crystallites. The nucleation process perhaps depends on the differences in the polyethylene chain segments. The bulky pendent group in LLDPE seems to severely impede the chain mobility and distinguishes itself from HDPE specifically in its nucleation behavior. Whereas mainly the linear polyethylene segments undergo crystallization for both the HDPE and LLDPE, and they show similar growth of crystallites. Thus, it is much probable that the individual seed crystallites (individual nuclei) merge together to form cocrystallites.

CONCLUSION

The melt blending of HDPE and LLDPE produces strong cocrystalline masses, which do not show any sign of segregation into the constituents, even when they are kept at sufficiently high temperature for a prolong period. On the contrary, they undergo cocrystallization, manifesting a singlet isothermal crystallization exotherm throughout the blends of different compositions. The Avrami exponent (n) comprises two fractions, as follows: the nucleation part ($n_{nucleation}$), and the growth part (n_{growth}) of crystallites. The nucleation part of the Avrami exponent is a blend-composition-dependent part, while the growth part of it is blend-composition-independent. The Avrami exponent also entails that the merging of individual nuclei of HDPE and LLDPE occurs to form cocrystallites.

The crystallites are unique in each blend formulation. This uniqueness in the conformation of crystallites at different blend compositions, as well as their pure constituting constituents, may be responsible for their characteristics light scattering pattern. The two-dimensional crystallites are apparent all through the blend compositions. The HDPE shows disklike crystallites, while the LLDPE and 80% LLDPE-containing blend possess sheaflike crystallites. Whereas the 35 and 50% LLDPE-containing blends show platelike conformation of crystallites.

The crystallization rate is relatively independent on the blend composition. However, the number and size of crystallites greatly explain the variation of crystallization rate constant. Grossly, it is seen that the large crystalline interface to the amorphous phase pool is either due to the presence of a large number of crystallites or is due to their bigger size and manifest faster crystallization.

The percentage of crystallinity is seen to vary in three ranges of blend compositions. In the HDPE-rich and LLDPE-rich region, the percentage of crystallinity is seen to decrease with the increase in LLDPE content, whereas the percentage of crystallinity remains almost constant in the middle region of blend composition. Being exclusive in nature to the percentage of crystallinity, $t_{1/2}$ is also seen to vary in the three regions but in the opposite manner.

The author thanks the Council for Scientific and Industrial Research, Pusa, New Delhi, India, for providing financial assistance to carry out this work.

REFERENCES

1. P. Vadhar and T. Kyu, *Polym. Eng. Sci.,* **27,** 202 (1987).
2. S. Hu, T. Kyu, and R. S. Stein, *J. Polym. Sci., Polym. Phys. Ed.,* **25,** 71 (1987).
3. A. K. Gupta, S. K. Rana, and B. L. Deopura, *J. Appl. Polym. Sci.,* **42,** 719 (1992).
4. T. Hashimoto, Y. Murakami, N. Hayashi, and K. Kawai, *Polym. J.,* **6,** 132 (1974).
5. W. Chu and R. S. Stein, *J. Polym. Sci.,* **A-2,** 489 (1970).
6. *Atlas of Polymer Morphology,* A. E. Woodward, Ed., Hanser Publishers, Vienna, 1988, Chap. 4.

7. *High Modulus Polymers,* A. E. Zachariades and R. S. Porter, Eds., Marcel and Dekker, Basel, 1988, Chap. 9.
8. *Self-Order and Form in Polymeric Materials,* A. Keller, M. Wavner, and A. H. Windle, Eds., Chapman and Hall, London, 1995, Chap. 1.
9. A. Avrami, *J. Chem. Phys.,* **7,** 1103 (1939).
10. A. Avrami, *J. Chem. Phys.,* **8,** 212 (1940).
11. A. Avrami, *J. Chem. Phys.,* **9,** 177 (1941).
12. F. V. Evans, *Trans. Faraday Soc.,* **41,** 365 (1945).
13. L. B. Morgan, *Philos. Trans. R. Soc., London, Ser. A,* **248,** 13 (1954).
14. L. Mandelkern, *Chem. Rev.,* **56,** 930 (1956).
15. A. Jezorney, *Polymer,* **19,** 1142 (1948).
16. J. N. Hay and Z. J. Perzekop, *J. Polym. Sci., Polym. Phys. Ed.,* **16,** 81 (1978).
17. J. N. Hay and P. J. Mills, *Polymer,* **23,** 1380 (1982).
18. J. Rabesiaka and A. I. Kovacs, *J. Appl. Phys.,* **32,** 2341 (1961).